Removal of toxic elements from aqueous solution using bentonite modified with L-histidine

E. N. Bakatula, E. M. Cukrowska, I. M. Weiersbye, L. Mihaly-Cozmuta and H. Tutu

ABSTRACT

This study proposes the use of bentonite modified with L-histidine for the removal of Cu, Co, Cr, Fe, Hg, Ni, U and Zn from aqueous solutions such as those impacted by acidic drainage. The surface areas of natural bentonite and bentonite–histidine were 73.8 and 61.2 $m^2 g^{-1}$, respectively. Elemental analysis showed an increase in the amount of carbon (0.258%) and nitrogen (0.066%) for the bentonite–histidine. At a fixed solid/solution ratio, the operating variables affecting the adsorption of metal ions from aqueous solution such as pH, initial concentration, contact time and temperature were studied in batch mode. The Freundlich isotherm model yielded a better fit than the Langmuir for the adsorption of Cu, Co, Ni and Zn, implying adsorption on a heterogeneous surface. Adsorption kinetics followed a pseudo-second-order model, suggesting chemisorption as the rate-limiting step. The apparent activation energy was greater than 40 kJ mol^{-1} for Cu, Zn, Ni, Co and U, which is characteristic of a chemically controlled reaction. Thermodynamic constants ΔG and ΔH showed that the adsorption of metals was endothermic and spontaneous. Adsorption of heavy metals onto bentonite–histidine was efficient at low pH values, meaning that the adsorbent could be useful for remediating acid mine water.

Key words | adsorption, bentonite–histidine, kinetics, toxic elements, thermodynamics

E. N. Bakatula
E. M. Cukrowska
H. Tutu (corresponding author)
Molecular Sciences Institute,
School of Chemistry,
University of the Witwatersrand,
Private Bag X3,
WITS 2050,
Johannesburg,
South Africa
E-mail: *hlanganani.tutu@wits.ac.za*

I. M. Weiersbye
School of Animal, Plant and Environmental Sciences,
University of the Witwatersrand,
Private Bag X3, WITS 2050,
Johannesburg,
South Africa

L. Mihaly-Cozmuta
Technical University of Cluj Napoca, North University Center Baia Mare,
76, Victoriei Street,
430122 Baia Mare,
Romania

INTRODUCTION

The increasing health and environmental problems resulting from the dispersion of heavy metals into the environment as a result of human activities such as mining, industrial and agricultural activities have become of universal concern. Owing to the highly toxic and complex composition of wastewaters from such activities, this has led to very difficult and expensive treatment processes. It is therefore necessary to find cheaper and simple decontamination methods.

Traditional processes used for treating effluents that contain heavy metals include: ion exchange (Mohsen-Nia *et al.* 2007), reverse osmosis (Charerntanyarak 1999), chemical coagulation and precipitation (Landáburu-Aguirre *et al.* 2009), ultrafiltration (Jiang *et al.* 2010) and adsorption (Adebowale *et al.* 2008). From literature, liquid-phase adsorption is one of the most popular methods for the removal of pollutants from wastewater since proper design of the adsorption process will produce a high-quality treated effluent (Crini 2005). Different adsorbents have been employed in the process of adsorption, including activated charcoal, kaolinite, natural and synthetic zeolites, rice husks and clays (Ouki & Kavannagh 1999; Abollino *et al.* 2003; Gupta & Bhattacharyya 2005; Vieira *et al.* 2010; Neto *et al.* 2012), among others. Clays have properties such as high cation exchange capacity; they are easily available and are low cost adsorbents that can be recycled and reused for subsequent cycles.

Bentonite is an alumino-silicate clay, derived from weathered volcanic ash and largely composed of montmorillonite (70–90%). It is known for its excellent sorption properties towards metal cations and is widely used for the purification of wastewaters. Moreover, the surface modification of bentonite with different organic and inorganic cations such as amino acids leads to more efficient sorptive systems. Natural clays are not very effective by themselves in different applications and as such modification may be required to make them specific for adsorption and catalytic properties. Considering the mechanisms of clay–organic interactions, the organic compound can bind the surface

doi: 10.2166/wst.2014.450

and/or penetrate into the interlayer space of clay minerals as a ligand (Balek *et al.* 2002).

Several studies have been conducted using bentonite clay as an adsorbent for metals (Inglezakis *et al.* 2007; Bertagnolli *et al.* 2011; Galindo *et al.* 2013).

L-histidine ($C_6H_9N_3O_2$) is one of the organic compounds produced by microorganisms such as fungi and yeast and interacts with the clay mainly through the imidazole group. Studies revealed that the adsorption capacity of bentonite could be enhanced by surface modification using organofunctional coupling agents (de Mello *et al.* 2008).

Batch experiments are commonly used in laboratory to evaluate the treatment of small volumes of effluents, providing preliminary information based on the kinetic and thermodynamic studies, which are helpful for selecting optimum operating conditions for the full-scale batch and fixed-bed process.

The aim of this paper was to assess the adsorption of Cu, Co, Fe, Hg, Ni, Zn and U from single-element aqueous solutions using bentonite treated with L-histidine. Kinetic parameters were calculated to determine the sorption mechanisms and potential rate-controlling steps, involved in the adsorption processes. Adsorption isotherms, Langmuir and Freundlich, were applied to the equilibrium data with the objective of describing the principal interactive mechanisms involved in the removal process. Thermodynamic parameters were calculated at different temperatures. The effects of pH and metal concentration on the adsorption were also assessed.

MATERIALS AND METHODS

Preparation of bentonite–histidine

The natural bentonite used as adsorbent in the present study, a gray fine powder (particle size <2 mm), was supplied by Sigma-Aldrich (Pty) Ltd South Africa. The adsorbent was oven dried for 24 h at 60 °C before the experiments. Ten grams of natural bentonite interacted at 60 °C for 48 h with 100 mL of a solution containing 1.55 g of L-histidine hydrochloride at pH 8. The synthesized sorbent was washed several times with de-ionized water to remove any unreacted L-histidine. The bentonite–histidine was re-suspended in de-ionized water, stirred for about 1 h at room temperature and separated by filtration. The suspension was dried in the oven for 24 h at 60 °C. L-Histidine was analyzed before and after reaction using the ninhydrin method as described by Fisher *et al.* (1963). Absorbance was read with a spectrophotometer, Jenway 6300.

All dried samples were pulverized to fine particles and stored prior to subsequent studies.

Characterization of natural and functionalized bentonite

Natural and functionalized bentonite was characterized using a Bruker D_2 Phaser (Karlsruhe, Germany) X-ray diffractometer using Ni-filtered Cu Kα radiation. The chemical composition of bentonite was determined using X-ray fluorescence (XRF).

The thermal stability of natural bentonite was assessed with thermogravimetric (TG) analysis carried out on a Perkin-Elmer Diamond DTG/TDA (derivative thermogravimetric/thermal differential analysis) analyzer. The temperature range was from 50 to 400 °C at a heating rate of 10 °C min^{-1} under nitrogen flow rate of about 20 mL min^{-1}. The Fourier transform infrared (FTIR) spectra were obtained on a Tensor 27 (Bruker, Germany) device in the range of 4,000–400 cm^{-1}. The LECO CHNS-932 analyzer was used to determine the amount of C, H and N in natural and modified bentonite.

The cation exchange capacity was determined by the $BaCl_2$ compulsive exchange method (Gillman & Sumpter 1986). The specific surface area and pore size distribution of the natural bentonite were determined via N_2 adsorption/desorption isotherms according to the BET (Brunauer–Emmett–Teller) surface analysis technique using a Micromeritics Tristar surface area and porosity analyzer. Samples (0.2 g) were degassed in N_2 at 400 °C for 4 h prior to analysis using a Micromeritics Flow Prep 060 sample degas system. The surface areas and pore size distributions were then obtained at −196 °C (Brunauer *et al.* 1938).

Certified reference materials were used for validating the methods used.

Preparation of standard solutions

The synthetic metal ion solutions containing Co^{2+}, Cu^{2+}, Fe^{3+}, Cr^{3+}, Hg^{2+}, Ni^{2+}, UO_2^{2+} and Zn^{2+} were prepared by weighing appropriate amounts of their nitrate salts: $Cu(NO_3)_2.3H_2O$, $Co(NO_3)_2.6H_2O$, $Ni(NO_3)_2.7H_2O$, $Cr(NO_3)_3.9H_2O$, $Zn(NO_3)_2.6H_2O$, $UO_2(NO_3)_2.6H_2O$, $Fe(NO_3)_3.9H_2O$, $Hg(NO_3)_2.H_2O$, which were sufficiently dried to enable preparation of standard solutions of 1,000 mg L^{-1}. Appropriate aliquots were taken from these standards for subsequent dilution to the desired concentration

level. The solutions were acidified using 1 mol L^{-1} HNO_3 to avoid the precipitation of the metals, and stored in a refrigerator at 4 °C prior to the relevant experiments.

Batch sorption studies

Batch sorption tests were conducted by mixing 1 g of bentonite–histidine with 50 mL of synthetic solutions containing the desired concentration of heavy metal ions, at 25 ± 1 °C. The pH of the solution was adjusted by addition of dilute HNO_3 or NaOH solution. The mixture was agitated in 250 mL plastic bottles at 150 rpm and then filtered. The final metal concentration in the aqueous phase was determined using inductively coupled plasma – optical emission spectroscopy. Data obtained from batch adsorption tests were used to calculate the amount of metal ion adsorbed on the adsorbent q_e (mg g^{-1}) using the following mass balance equation (Equation (1)):

$$q_e = \frac{(C_o - C_t)V}{M} \tag{1}$$

where q_e (mg g^{-1}) is the adsorption capacity; C_o and C_e (mg L^{-1}) are the initial and equilibrium metal concentrations, respectively; V is the solution volume (L) and M is the amount of adsorbent (g).

The distribution of coefficient, K_d (L mol^{-1}), was calculated using the following relationship (Equation (2)):

$$K_d = \frac{q_e}{C_e} \tag{2}$$

Adsorption isotherms

To identify the mechanism of the adsorption process, the adsorption of metal ions was determined as a function of equilibrium concentrations for the initial metal concentration ranging from 50 to 500 mg L^{-1}. The Langmuir and Freundlich isotherm models were used to fit the experimental data.

The Langmuir model (Langmuir 1918) was originally developed assuming monolayer adsorption on a surface of the adsorbent with a finite number of adsorption sites.

It is expressed by Equation (3).

$$q_e = \frac{q_m b C_e}{1 + bC_e} \tag{3}$$

The Freundlich model assumes that adsorption takes place on heterogeneous surfaces of the adsorbent. This model is presented in Equation (4).

$$q = KCe^n \tag{4}$$

q_m (mg g^{-1}) is the monolayer adsorption capacity and b (L mg^{-1}) is the adsorption equilibrium constant related to the free energy of adsorption. K_F ($mg^{1-(1/n)}$ $L^{1/n}$ g^{-1}) and n are empirical Freundlich constants.

Adsorption kinetics

Kinetic tests were carried out by mixing 25 g of clay adsorbent with 500 mL of a solution containing 100 mg L^{-1} of metal ions. Samples were withdrawn from the shaker at different time intervals and centrifuged for 10 min. The amount of metal ion adsorbed on the adsorbent (q_e) was calculated using Equation (1).

The pseudo-first-order, pseudo-second-order and intraparticle diffusion kinetic models were applied to experimental data with the purpose of evaluating the adsorption process.

The pseudo-first-order model is presented in Equation (5) (Lagergren 1898).

$$\log(q_e - q_t) = \log(q_e) - \frac{k_1.t}{2.303} \tag{5}$$

The pseudo-second-order model is expressed by Equation (6) (Ho & McKay 1998).

$$\frac{t}{qt} = \frac{1}{k_2 qe^2} + \frac{1}{qe}\ t \tag{6}$$

where q_t and q_e are the adsorbed amounts (mol kg^{-1}) at time t (experimentally obtained) and at equilibrium, respectively, and k_1 and k_2 are the rate constants.

The intraparticle diffusion model is characterized by a linear relationship between the amounts adsorbed (q_t) and the square root of the time and is expressed as follows (Ho & McKay 1998):

$$q_t = K_p \cdot t^{0.5} + I_d \tag{7}$$

The two parameters can be obtained from the intercept of the plot of q_t versus $t^{0.5}$. The constant I_d is used to examine the relative significance of the two transport mechanisms of the solute, intraparticle diffusion and external mass transfer.

Thermodynamic parameters

Experiments were carried out to determine the effect of temperature on metal adsorption by bentonite–histidine. Two grams of adsorbent were added to 100 mL of solution containing 100 mg L^{-1} of metal. The mixture was shaken in a temperature-controlled room at 291, 295, 299 and 303 K at 150 rpm for the equilibrium time. The solution pH was fixed at 3. The thermodynamic parameters for the adsorption process including Gibb's free energy change (ΔG, J mol^{-1}), enthalpy change (ΔH, kJ mol^{-1}) and entropy change (ΔS, J mol^{-1} K^{-1}) were calculated using Equations (8) and (9) (Vadivelan & Kumar 2005).

$$\ln K_d = \frac{\Delta H}{RT} + \frac{\Delta S}{R} \tag{8}$$

$$\Delta G = \Delta H - T\Delta S \tag{9}$$

The value of ΔS and ΔH can be obtained from the slope and intercept of the plot between $\ln(K_d)$ versus $1/T$.

The Gibbs free energy change ΔG (kJ mol^{-1}) can be calculated using the relation:

$$\Delta G = -RT \ln K_d \tag{10}$$

Activation energy refers to the minimum kinetic energy that must be supplied to the system in order for a chemical process to take place. In adsorption processes, the activation energy can be obtained using the Arrhenius equation (Levine & Slade 1988) as follows:

$$\ln \frac{k_2(T_2)}{k_1(T_1)} = -\frac{\mathrm{Ea}}{R}\left(\frac{1}{T_2} - \frac{1}{T_1}\right) \tag{11}$$

where k_1 and k_2 are the apparent rate constants; Ea is the activation energy; and R and T are the universal gas constant (8.314 J mol^{-1} K^{-1}) and temperature (K), respectively.

The accuracy of the adsorption models was demonstrated using two statistical parameters, namely, the correlation coefficient (R^2) and the normalized standard deviation Δq(%) as presented in Equation (12).

$$\Delta q(\%) = 100\sqrt{\frac{\sum_{i=1}^{n}\left[\left(q_{\mathrm{exp}} - q_{\mathrm{calc}}\right)/q_{\mathrm{exp}}\right]^2}{n-1}} \tag{12}$$

RESULTS AND DISCUSSION

Characterization of natural and modified bentonite

Mineralogical and elemental composition

The mineralogical composition of natural bentonite determined by XRF was (%): SiO_2 52.26, Al_2O_3 17.25, Fe_2O_3 0.53, FeO 4.25, MnO 0.07, MgO 3.67, CaO 2.05, K_2O 1.38, Na_2O 0.35, TiO_2 0.4, P_2O_5 0.09, and loss on ignition was 17.72%. The surface area of natural bentonite was higher than that for functionalized bentonite. The amount of L-histidine loaded on bentonite was 650 μmol g^{-1}. The BET surface area significantly decreased after modification due to coverage of the pores of natural bentonite. The results showed an increased amount of carbon (0.742%), hydrogen (0.258%) and nitrogen (0.744%) in the bentonite–histidine compared to natural bentonite.

The X-ray diffraction (XRD) pattern of natural bentonite is presented in Figure 1. The bentonite was found to be crystalline, and mainly consisting of sillimanite, $Al_2(SiO_4)O$, with the highest peak occurring at a value of 32. Most of the peaks are of aluminum silicate $(Al_xSi_{1-x})O_2$ occurring in different phase, i.e., kyanite and andalusite.

Thermal analysis

Thermal analysis of natural bentonite gave information about its thermal reactions and stability. The TG/DTG curve showed a weight loss between 25 and 150 °C, corresponding to the desorption of internal and external water of hydration (100–91%). Less weight loss was observed above 500 °C, proving that bentonite is thermally stable over a temperature of 500 °C.

FTIR analysis

The modification of natural bentonite was verified by FTIR spectra.

The bonds between bentonite and histidine were observed from the peaks at 3,902 and 3,734 cm^{-1} (probably N—H stretchings caused by NH_2) and 3,446 cm^{-1} (carbonyl O—H band) invisible in the structure because it fits into the O—H stretchings of histidine. The band at 1,507–1,489 cm^{-1} was due to N—H bendings while that at 1,457 cm^{-1} was due to C=N stretching. The C=O carbonyl band expected at 1,630–1,640 cm^{-1} fitted into the O—H bending of water in bentonite. As a result of this, the O—H bending of bentonite appeared different, a phenomenon that could be seen from

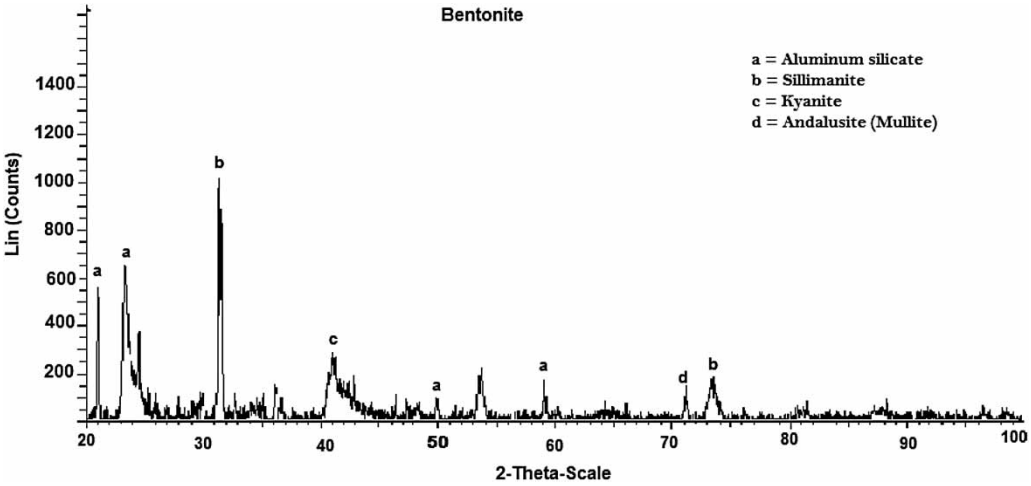

Figure 1 | XRD spectrum of bentonite powder.

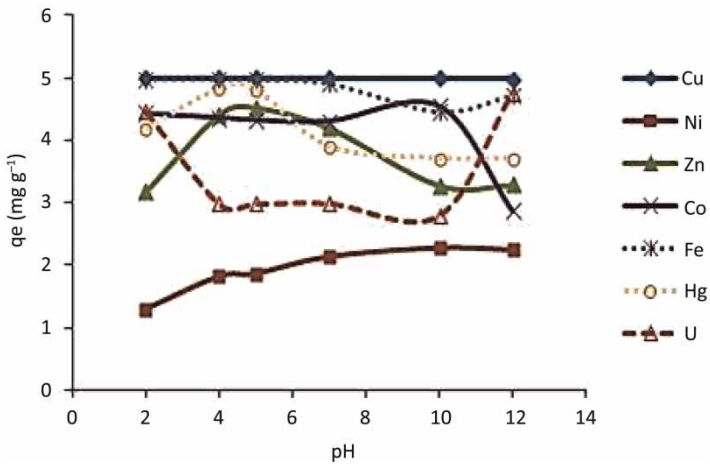

Figure 2 | Effect of initial pH on the adsorption of Cu, Ni, Zn, Co, Fe, Hg and U onto bentonite–histidine ($C_i = 100$ mg L^{-1}, temp = 298.15 ± 1 K, contact time = 12 h).

the spectra. The C—O stretching band was hidden by the H–OH peak. From these results, it seems that bentonite interacts with the NH_2 groups of histidine. In addition, the band at 1,507 cm^{-1} represented NH_3^+ bending. Consequently, it seemed like the bentonite structure interacted with the NH_2 group of histidine. The sorption of an organic material onto a negatively charged surface is a complex process involving both cation exchange and hydrophobic bonding (Wieczorek *et al.* 2003).

Adsorption studies

Effect of solution pH

The effect of pH on adsorption of metals onto bentonite–histidine was studied in the pH range 2–12. The results are shown in Figure 2.

The results showed high adsorption capacity at low pH for Co, Zn, Fe, Hg and U. An increase with pH was observed for Ni whereas the adsorption rate was constant at all range of pH for Cu. The formation of complexes between the metal ions and bentonite–histidine depends on the amine groups present on the adsorbent. The rate of adsorption increases with increasing amine groups on the structure.

At pH < 4, histidine acts as a proton 'shuttle', the amine group is protonated and, in the presence of the silicon oxide, zwitterions are formed, which are less subjected to leaching compared to metal ions.

At high pH, some of the metals tend to form precipitates thus increasing metal removal. At higher pH regimes, the metals form soluble hydroxides that persist in solution, thus decreasing adsorption, e.g. Co, Zn and Hg. The high pH also leads to deprotonation of the amine groups on histidine, resulting in negative charges that would likely repel

Table 1 | Langmuir and Freundlich parameters for metal ion adsorption on bentonite–histidine

	Fe	Cu	Co	Hg	Ni	Zn	U
Langmuir isotherm							
q_m (mol kg^{-1})	0.268	0.387	0.428	0.064	0.379	0.459	0.086
b	461.5	892.1	525.4	155.7	493.1	878.2	243.5
Δq (%)	74.55	56.76	53.11	81.50	58.19	49.61	79.47
R^2	0.999	0.941	0.967	0.976	0.984	0.931	0.988
Freundlich isotherm							
K_f	1.200	14.25	13.17	3.345	9.350	26.53	7.471
n	4.800	1.886	1.797	1.918	1.944	1.641	1.666
Δq (%)	24.65	11.07	7.204	43.71	10.70	10.03	21.62
R^2	0.927	0.986	0.994	0.784	0.986	0.989	0.948
Distribution coefficient							
K_d	9,388	1,776	894.3	345.9	930.2	1,333	58.15

the negative hydroxide complexes. Fe and U on the other hand showed an increase in adsorption beyond pH 10, the reason for which is not apparent from the study and would require further pursuit. This observation is similar to another in a separate study by the authors (Bakatula *et al.* 2014) in which the presence of Fe was found to enhance the uptake of U onto algal biomass.

Adsorption isotherms

The isothermic parameters calculated for the Langmuir and Freundlich models are presented in Table 1. Based on correlation coefficients (R^2 values), the adsorption process was better described by the Freundlich model, except for Fe and Hg, which were better described by the Langmuir isotherm.

The maximum adsorption capacities (mol kg^{-1}) obtained from the Langmuir isotherm are as follows: Zn (0.459) > Co (0.428) > Cu (0.0.387) > Ni (0.379) > Fe (0.268) > U (0.086) > Hg (0.064). However, large errors (Δq%) were obtained for the Langmuir isotherm in the assessment of the maximum adsorption capacity. The selectivity obtained for the distribution coefficient (K_d) is as follows: Fe(9,388) > Cu (1,776) > Zn (1,333) > Ni (930.2) > Co (894.3) > Hg (345.9) > U (58.15). The values of the distribution coefficients are high for Fe and Cu, indicating increased affinity of these metals for the adsorbent.

Adsorption kinetics

Kinetic tests were performed using monocomponent solutions. A rapid adsorption of metal ions occurred within 30 min followed by a slow uptake for 12 h. The adsorption capacity for U and Hg increased significantly in modified bentonite. The sorption of metals onto natural bentonite followed the sequence: Fe > Cu >Zn, Ni >Co >U > Hg, whereas in bentonite–histidine the sequence was: Fe >Hg > Cu >U > Co > Zn > Ni. The initial stage of fast adsorption was found by Inglezakis *et al.* (2004) to correspond to ion exchange in micro-pores. Furthermore, the driving force for adsorption, which is the concentration difference between the bulk solution and the solid–liquid interface, is initially very high and this also results in a higher adsorption rate. Kinetic models were used to fit the data, and their parameters are summarized in Table 2.

The adsorption process was found to be defined by high correlation coefficients (R^2 values close to unity), implying that adsorption was via chemisorption (strong chemical bond between the metal and adsorbent).

The rate constants for the pseudo-second-order model (k_2) were found to be in the range 0.251–3,847 g (mg min)$^{-1}$ with a higher rate constant k_2 obtained for Fe.

The initial rate (K_p) values calculated from the intraparticle diffusion model ranged from 1×10^{-3} to 5×10^{-3} mol kg^{-1} min$^{0.5}$.

Adsorption thermodynamics

Thermodynamic parameters such as enthalpy change (ΔH), Gibbs free energy (ΔG), entropy change (ΔS) and activation energy (Ea) for the sorption of the metals onto bentonite–histidine were calculated at different temperatures and the results are presented in Table 3.

Table 2 | Kinetic constants for the adsorption of metals onto bentonite–histidine

	Fe	Cu	Co	Hg	Ni	Zn	U
Pseudo-first-order							
q_e (mol kg^{-1})	0.001	0.006	0.013	0.001	0.027	0.011	0.001
K_1	0.029	0.009	0.010	0.009	0.005	0.020	0.008
Δq (%)	92.55	88.24	81.24	91.38	69.97	79.49	88.77
R^2	0.605	0.628	0.811	0.493	0.875	0.940	0.602
Pseudo-second-order							
q_e (mol kg^{-1})	0.089	0.077	0.073	0.0246	0.0753	0.068	0.020
K_2	3,847	3.483	1.353	31.53	0.251	3.365	9.099
Δq (%)	0.002	1.433	2.196	1.070	16.28	0.999	3.635
R^2	1.000	0.999	0.999	1.000	0.994	1.000	0.999
Intraparticle diffusion							
I_d	0.036	0.028	0.022	0.010	0.012	0.024	0.007
K_p	0.005	0.004	0.004	0.001	0.003	0.004	0.001
Δq (%)	29.27	29.93	31.05	29.44	34.50	29.98	29.99
R^2	0.721	0.747	0.814	0.723	0.895	0.770	0.740

Table 3 | Thermodynamic parameters for the sorption of metals onto bentonite–histidine

	Ea kJ mol^{-1}	ΔH kJ mol^{-1}	ΔS J (mol K)$^{-1}$	ΔG kJ mol^{-1}			
	295 K	295 K	295 K	291.15 K	295.15 K	299.15 K	303.15 K
Cu	52.49	122.4	479.1	−14.52	−14.99	−15.63	−17.31
Ni	57.46	132.3	496.2	−14.18	14.28	−12.53	−12.39
Zn	74.68	176.1	662.5	−14.18	−18.3	−16.61	−16.79
Co	63.42	146.1	557.7	−19.15	−19.56	−16.07	−16.30
Hg	33.72	77.7	315.4	−16.01	−15.75	−14.95	−14.15
U	104.4	239.6	892.3	−13.22	−19.263	−20.27	−20.29
Fe	10.82	350.4	1,257	−18.16	−16.74	−16.34	−16.12

The values for activation energies were calculated from the Arrhenius equation (Equation (11)) and were found to be elevated (>40 kJ mol^{-1}) for Cu, Zn, Ni, Co and U implying adsorption via chemisorption, thus substantiating the previous observation for kinetic modeling. Ea values ranged from 10 to 33 kJ mol^{-1} for Fe and Hg suggesting that adsorption occurs via physisorption. A reaction is classified as physisorption when the Ea ranges between 5 and 40 kJ mol^{-1}, whereas chemisorption has an Ea value between 40 and 800 kJ mol^{-1} (Boparai *et al.* 2010).

These metals were likely bound to sites of low energy. The positive values of ΔH indicated that the sorption is an endothermic process; that is, the enthalpy increases with the temperature. The negative values of ΔG indicate the feasibility and spontaneity of the adsorption process. The thermodynamic parameters for bentonite–histidine at each temperature were greater than those obtained at the same temperature for natural bentonite. This could be due to complex formation between the metal ions and amine groups attached.

As shown in Table 3, ΔS values are positive for all metals studied, implying their randomness at the interface of the sorbent. Fe and U showed very high entropy values of 1,257 and 892.3 J mol K^{-1}, respectively. It was observed that the rate of adsorption of the metals increased with increasing temperature, with Fe being the least affected whereas mercury was the most affected. Positive ΔS values represent an increase in randomness at the interface

between the solid and the solution during fixation of metals on the active sites of the adsorbent (Huang *et al.* 2011).

CONCLUSION

The study showed that the adsorption capacity of bentonite can be enhanced by modification of the surface using a biological component such as histidine. This can be found in organisms such as algal and fungal biomass that are common in aqueous solutions in the natural environment. The hybrid organic–inorganic material can provide an alternative low cost material for the treatment of polluted aqueous solutions such as mine wastewater and possibly for the recovery of precious metals from such effluent. The metal adsorption rate for bentonite–histidine was found to be greater than that for natural bentonite at high metal concentrations due to the structure of bentonite–histidine. Adsorption capacity ($mg\,g^{-1}$) for bentonite–histidine increased by 9%, 12%, 8%, 22%, 26%, 50%, 52% and 25% for Cu, Co, Cr, Fe, Hg, Ni, Zn and U, respectively. Complexation and ion exchange on the bentonite–histidine surface contribute to elevated adsorption capacity. Bentonite–histidine was more efficient in metal adsorption mostly at low pH due to the presence of N–H.

In the commercial sense, chemical modification by amine coupling agents may be a useful tool for the preparation of new adsorbents with high adsorption capacities and selectivity towards metals in wastewater such as from acidic mine leachates. In the natural environment, the findings point to the possibility of reaction of biological components exuded by biomass with natural adsorbents such as bentonite or clay that are present in aqueous systems. Such reactions will lead to improved adsorption capacities of the adsorbents and thus improved natural attenuation of metals.

ACKNOWLEDGEMENTS

The authors would like to thank the National Research Foundation and the Carnegie Foundation for financial support.

REFERENCES

Abollino, O., Aceto, M., Malandrino, M., Sarzanini, C. & Mentasti, E. 2003 Adsorption of heavy metals on Na-montmorillonite. Effect of pH and organic substances. *Water Res.* **37** (7), 1619–1627.

Adebowale, K. O., Emmanuel, E. I. & Olu-Owolabi, B. I. 2008 Kinetic and thermodynamic aspects of the adsorption of Pb^{2+} and Cd^{2+} ions on tripolyphosphate-modified kaolinite clay. *Chem. Eng. J.* **136** (2–3), 99–107.

Bakatula, E. N., Cukrowska, E. M., Weiersbye, I. M., Mihaly-Cozmuta, L., Peter, A. & Tutu, H. 2014 Biosorption of trace elements from aqueous systems in gold mining sites by the filamentous green algae (*Oedogonium* sp.). *J. Geochem. Expl.* (in press). dx.doi.org/10.1016/j.gexplo.2014.02.017.

Balek, V., Malek, Z., Ehrlicher, U., Györyová, K., Matuschek, G. & Yariv, S. 2002 Emanation thermal analysis of TIXOTON (activated bentonite) treated with organic compounds. *Appl. Clay Sci.* **21** (5–6), 295–302.

Bertagnolli, C., Kleinübing, S. J. & Silva, M. G. C. 2011 Preparation and characterization of a Brazilian bentonite clay for removal of copper in porous beds. *Appl. Clay Sci.* **53** (1), 73–79.

Boparai, H. K., Joseph, M. & O'Carroll, D. M. 2010 Kinetics and thermodynamics of cadmium ion removal by adsorption onto nano zerovalent iron particles. *J. Hazard. Mater.* **186**, 458–465.

Brunauer, S., Emmett, P. H. & Teller, E. 1938 Adsorption of gases in multimolecular layers. *J. Am. Chem. Soc.* **60**, 309–319.

Charerntanyarak, L. 1999 Heavy metals removal by chemical coagulation and precipitation. *Water Sci. Technol.* **39** (10–11), 135–138.

Crini, G. 2005 Non-conventional low-cost adsorbents for dye removal: a review. *Bioresour. Technol.* **97** (9), 1061–1085.

de Mello, A., Sampaio, V., Ciminelli, T. & van der Luiz, V. 2008 Smectite organo-functionalized with thiol groups for adsorption of heavy metal ions. *Appl. Clay Sci.* **42**, 410–414.

Fisher, L. J., Buting, S. L. & Rosenberg, L. E. 1963 A modified ninhydrin colorimetric method for determination of plasma alpha-amino nitrogen. *Clin. Chem.* **9**, 573–581.

Galindo, L. S. G., Neto, A. F., da Silva, M. G. C. & Vieira, M. G. A. 2013 Removal of cadmium(II) and lead(II) ions from aqueous phase on sodic bentonite. *Mater. Res.* **16** (2), 515–527.

Gillman, G. P. & Sumpter, E. A. 1986 Modification to the compulsive exchange method for measuring exchange characteristics of soils. *Aust. J. Soil Res.* **24**, 61–66.

Gupta, S. S. & Bhattacharyya, K. G. 2005 Removal of Cd(II) from aqueous solution by kaolinite, montmorillonite and their poly (oxo zirconium) and tetrabutylammonium derivatives. *J. Hazard. Mater.* **128** (2–3), 247–257.

Ho, Y. S. & McKay, G. 1998 Kinetic model for lead(II) sorption onto peat. *Adsorpt. Sci. Technol.* **16** (4), 243–255.

Huang, R., Wang, B., Yang, B., Zheng, D. & Zhang, Z. 2011 Equilibrium, kinetic and thermodynamic studies of adsorption of Cd(II) from aqueous solution onto HACC-bentonite. *Desalination* **280** (1), 297–304.

Inglezakis, V. J., Loizidou, M. M. & Grigoropoulou, H. P. 2004 Ion exchange studies on natural and modified zeolites and the concept of exchange site accessibility. *J. Colloid Interface Sci.* **275**, 570–576.

Inglezakis, V. J., Stylianou, M. A., Gkantzoua, D. & Loizidoua, M. D. 2007 Removal of Pb(II) from aqueous solutions by using clinoptilolite and bentonite as adsorbents. *Desalination* **210** (1–3), 248–256.

Jiang, M. Q., Jin, X. Y., Lu, X. & Chen, Z. L. 2010 Adsorption of Pb(II), Cd(II), Ni(II) and Cu(II) onto natural kaolinite clay. *Desalination* **252** (1–3), 33–39.

Lagergren, S. 1898 Zur theorie der sogenannten adsorption gelöster stoffe. *Kungliga Svenska Vetenskapsakademiens. Handlingar Band* **24** (4), 1–39.

Landáburu-Aguirre, J., García, V., Pongrácz, E. & Keiski, R. L. 2009 The removal of zinc from synthetic wastewaters by micellar-enhanced ultrafiltration: statistical design of experiments. *Desalination* **240** (1–3), 262–269.

Langmuir, I. 1918 The adsorption of gases on plane surfaces of glass, mica and platinum. *J. Am. Chem. Soc.* **40**, 1361.

Levine, H. & Slade, L. 1988 Water as a plasticizer: physico-chemical aspects of low-moisture polymeric systems. In: *Water Science Reviews*, Vol. 3 (F. Franks, ed.). Cambridge University Press, Cambridge, pp. 79–185.

Mohsen-Nia, M., Montazeri, P. & Modarress, H. 2007 Removal of Cu^{2+} and Ni^{2+} from waste water with a chelating agent and reverse osmosis processes. *Desalination* **217** (1–3), 276–281.

Neto, A. F., Vieira, M. G. A. & Silva, M. G. C. 2012 Cu(II) adsorption on modified bentonitic clays: different isotherm behaviors in static and dynamic systems. *Mater. Res.* **15** (1), 114–124.

Ouki, S. K. & Kavannagh, M. 1999 Treatment of metals-contaminated wastewaters by use of natural zeolites. *Water Sci. Technol.* **39** (10–11), 115–122.

Vadivelan, V. & Vasanth Kumar, K. 2005 Equilibrium, kinetics, mechanism and process design for the sorption of methylene blue onto rice husk. *J. Colloid Interface Sci.* **286** (1), 91–100.

Vieira, M. G. A., Neto, A. F., Gimenes, M. L. & Silva, M. G. C. 2010 Sorption kinetics and equilibrium for the removal of nickel ions from aqueous phase on calcined Bofe bentonite clay. *J. Hazard. Mater.* **177** (1–3), 362–371.

Wieczorek, M., Jesionowski, T. & Krysztafkiewicz, A. 2003 Influence of organic polymer modification on physicochemical properties of bentonites. *Physicochem. Probl. Miner. Process.* **37**, 131–140.

First received 18 August 2014; accepted in revised form 27 October 2014. Available online 8 November 2014